

Characterization of Liquefaction Resistance in Gravelly Soil : Large Hammer Penetration Test and Shear Wave Velocity Approach

Ping-Sien Lin^{*1}, Chi-Wen Chang¹, Wen-Jong Chang²

¹ Department of Civil Engineering, National Chung-Hsing University
Taichung, Taiwan, 402, ROC

Ph: (04) 2287-2221 ext 229; Fax: (04) 2286-2857

E-mail: pslin@dragon.nchu.edu.tw (Lin)

² Department of Civil Engineering, National Chi Nan University, Puli, Taiwan. 545

ABSTRACT

Gravelly soil is generally recognized to have no liquefaction potential. However, liquefaction cases are reported in central Taiwan in 1999 Chi-Chi Taiwan earthquake and in 1988 Armenia earthquake. Thus, further studies on the liquefaction potential of gravelly soil are warrent. Because large particles can impede the penetration of both SPT and CPT, shear wave velocity based correlation and large Hammer Penetration Test (LPT) are employed to evaluate the liquefaction resistance of gravelly soils. A liquefied gravelly deposit site during the Chi-Chi earthquake was selected for this research. In situ physical properties of soil deposits are collected from exploratory trenches. Instrumented Large Hammer Penetration Test (LPT) and shear wave velocity (V_s) measurements were performed to evaluate the liquefaction resistance. In addition, large-scale cyclic triaxial test on remolded gravelly soil samples (15 cm in diameter, 30 cm in height) were conducted to verify and improve LPT-based and V_s -based correlations. The results show that the Large Hammer Penetration Test and shear wave velocity methods are reasonably suitable for liquefaction assessment of gravelly soils.

Keywords: Gravelly soil, Liquefaction, Large Hammer Penetration Test, Shear wave velocity

1. INTRODUCTION

Soil liquefactions had been observed in central Taiwan area after 1999 Chi-Chi Earthquake ($M_w=7.6$). Although after earthquake investigations reveals that most liquefaction in Chi-Chi earthquake occurred in alluvium layers, which are composed of fine sand or fine sandy silt, liquefaction cases of gravelly soils were also reported in the Wufeng and Nantou Area. Gravelly soil is generally recognized to have no liquefaction potential. The reported cases of liquefied gravelly deposits in 1999 Chi-Chi Earthquake (Chu et al. [1]) and in 1988 Armenia earthquake (Yegian et al. [2]) raise concerns of liquefaction in saturated gravelly soils. Because there are very few well-documented case histories of liquefied gravelly deposits, research in studying the liquefaction mechanism and developing proper analyzing techniques for gravelly soils is warranted to minimize damage and loss caused by liquefaction of saturated gravelly soils.

Because the composition and fabric of gravelly deposits is different from other alluvium deposits, evaluation methods developed for sandy soils need be critically reviewed and modified to apply in gravelly soils. Currently, there is no well-recognized method for assessing the liquefaction resistance of gravelly soils. The conventional methods for evaluation of liquefaction resistance can be divided into two groups: (1) laboratory cyclic liquefaction tests (ex. Seed and Lee [3]), and (2) semi-empirical correlations with various in situ tests (ex. Seed et al. [4], Robertson and Wride [5], Andrus and Stokoe [6], Harder [7]). The oversize of gravelly particles makes cyclic triaxial testing apparatus with conventional specimen size not appropriate to gravelly soils. Additionally, conventional sampling techniques are not able to retrieve undisturbed, saturated, gravelly specimens. Large-scale cyclic triaxial testing apparatus with specimen diameter 150 mm is setup to performed series cyclic liquefaction tests in reconstituted gravelly specimens. Also, internal shear wave

velocity measurement system is integrated to the large-scale cyclic triaxial apparatus to measure the initial shear wave velocity of reconstituted specimens. The developed system is used to correlate the cyclic resistance of gravelly soils with gravels content and initial relative density. Also, the system provides laboratory verification for in situ shear wave velocity measurements and cyclic resistance evaluation based on initial shear wave velocity criteria.

Because large particles can impede the penetration of both Standard Penetration Test (SPT) and Cone Penetration Test (CPT), large Hammer Penetration Test (LPT) and shear wave velocity (V_s) based correlations are employed to evaluate the liquefaction resistance of gravelly soils. A liquefied gravelly site during the 1999 Chi-Chi earthquake was selected to perform the two in situ testing techniques. Series instrumented Large Hammer Penetration Tests (LPT) were conducted in the selected testing site. The instrumentation data were used to conduct corrections in transferred energy and casing friction. In situ shear wave velocity measurements were also performed at the same site. Both in situ testing methods are used to characterize the liquefaction resistance of gravelly soils. To verify the results, liquefaction resistances evaluated from both LPT and V_s are compared with field observation and laboratory testing results. All the efforts aim to find appropriate techniques for systematic assessing the liquefaction resistance of gravelly soils.

2. LITERATURE REVIEW

2.1 BPT-based Correlation

Because the particle size of gravels in gravelly soil deposits can impede the penetration of both SPT and CPT, the generally used CPT- and SPT-based correlations for liquefaction resistance evaluation are not applicable for gravelly deposits.

Consequently, the Becker Hammer Penetration (BPT) technique was selected as an alternative for field penetration tests. The relationship between blow counts of BPT (BPT- N_b) and blow counts of SPT (SPT-N) for 30 cm penetration was studied.

An earlier study to the relationship between BPT and SPT was conducted in British Columbia, Canada. The results showed a 1: 1 linear relationship between BPT- N_b and SPT-N values as shown in Figure 1. However, that study did not consider the effects of driving energy of the diesel hammer, diesel hammer combustible conditions, and the friction between soil and pile. Harder and Seed ([8]) recommended that the BPT- N_b should be corrected regarding to the bounce chamber pressure and the reduced combustion efficiencies while correlated the BPT- N_b and SPT-N values based on the fact that the driving energy of ram and the closed bounce chamber pressure are closely related. Harder and Seed [8] analyzed the bounce chamber pressure corrected BPT- N_b (BPT- N_{bc}) and energy corrected SPT-N (SPT- N_{60}) values from several research sites and proposed the corrected BPT-SPT curve as shown in Figure 2.

Sy and Campanella [9] point out that the casing friction should be considered in the correction of blow count as well as transferred energy. A strain gauge and an accelerometer were installed on the Becker casing to monitor the strain, stress, and acceleration of the casing. The peak force, peak velocity, and the percentage of the measured maximum transferred energy with respect to the hammer effective energy (ENTHRU) are calculated using the peak acceleration and acceleration-time history. The ENTHRU is obtained by integrating the product of force and velocity through the entire time elapse. The N_{b30} value, which corrected for 30% hammer effective energy, was computed by equation:

$$N_{b30} = N_b \frac{ENTHRU}{30} \dots\dots\dots (1)$$

where N_b = the measure blow count. The correlations among BPT- N_{b30} , SPT- N_{60} , and casing friction are shown in Figure 3. The casing frictional force is evaluated using the CAPWAP (GRL inc. [10]) program to simulate the pile driving system, casing, and soils in the field. Sy and Campanella [9] compares the measured blow count, N_b , bounce chamber pressure corrected blow count, N_{bc} , and the 30% energy corrected blow count, N_{b30} , and found that the effect of the casing frictional force is small within the top 30 m. Therefore, N_{b30} values can be correlated to SPT- N_{60} using the same correlations in Figure 2 but substituting N_{bc} to N_{b30} . Then, the correlations between cyclic resistance stress ratio (CRR) and SPT- N_{60} can be employed to assess the liquefaction resistance of gravelly soils.

2.2 V_s -based Correlation

Shear wave velocity is a basic engineering property of soils in earthquake site response analysis, which directly related to shear modulus at small shear strain level. The idea of using V_s as an index for characterizing liquefaction resistance is based on the factors (e.g. initial relative density, soil fabric, state of stress, age, and stress history) that affect liquefaction resistance also affect the in situ V_s (Andrus and Stokoe [6]). Using surface wave velocity measuring techniques, a shear wave velocity profile can be established without boring and penetration. The nondestructive, non-intrusive features make V_s -based approach an potentially attractive alternative for characterizing liquefaction resistance in gravelly soils. The best V_s -based correlation is proposed by Andrus and Stokoe [6]. The cyclic resistance stress ratio, CRR, is estimated by:

$$CRR = \frac{\tau_{ave}}{\sigma'_o} = a \left(\frac{V_{s1}}{100} \right)^2 + b \left[\frac{1}{(V_{s1}^* - V_{s1})} - \frac{1}{V_{s1}^*} \right] \dots\dots\dots (2)$$

where V_{s1} = overburden stress-corrected shear wave velocity, V_{s1}^* = limiting upper

value of V_{s1} ranging from 200 to 215 m/s depending on fines content, and a and b = curve fitting parameters ($a=0.022$, $b=2.8$ for gravelly soils). Because the shear wave velocity of gravelly soils is highly dependent on the particle gradation (Kokusho et al. [11]) and the soil density, the V_{s1}^* , a , and b parameters suggested by Andrus and Stokoe [6] need further investigation. The integrated internal shear wave velocity measurement system in large-scale cyclic triaxial apparatus is developed to verify the associated parameters.

2.3 Laboratory Cyclic Triaxial Liquefaction Test

Cyclic triaxial apparatus had been employed to characterize liquefaction resistance of granular soils since early 1960's (Seed and Lee [3]). Cyclic strength curve, which graphically expresses the relationship between density, cyclic stress amplitude, and number of cycles to initiate liquefaction, is established by series cyclic triaxial tests that cyclic loads are applied until liquefaction occurred. Although liquefaction resistance determined by laboratory cyclic triaxial liquefaction tests is less valuable in engineering practice because liquefaction resistance can be altered due to sample disturbance, laboratory cyclic triaxial liquefaction tests are still useful in quantitative assessment of factors affecting liquefaction.

Evans et al. [12] reveals that membrane compliance will affect the liquefaction resistance of uniformly graded gravels determined by cyclic triaxial tests. Evan and Zhou [13] conducted series conventional size triaxial liquefaction tests to quantify the effect of gravel content on the liquefaction resistance of sand-gravel composites. The results show that the increase in gravel content significantly increases the liquefaction resistance. Previous laboratory works are based on tests in conventional size (diameter=71 mm) specimens with particle size less than 10 mm. To overcome the size effect and boundaries limitation, a large-size (diameter=150 mm) cyclic triaxial

apparatus had been developed and employed in this study.

3. TESTING PROGRAM

3.1 Site Conditions

The liquefied site selected for this study is approximately 2 km from the ruptured fault of 1999 Chi-Chi earthquake and near Fu-Tin Bridge over the Dali River in Wufeng area. Liquefaction evidences had been observed after Chi-Chi earthquake (Chu et al. [1]). According to the boring data obtained from MAA Consultant Engineers [14], the ground water table is approximately 3.5m below the ground surface. Field investigation conducted by authors reveals that gravelly layer extended from ground surface to at least 23.5m deep. A thin layer of yellowish, silty, fine sand is interbedded within 2.1 to 7.0 m deep. The average fine content of interbedded silty sand is 21%. To collect more site details, an exploratory trench was excavated down to 7m deep. Soil profile from the trench excavation is shown in Table 1. A clay layer was found at 4m to 4.5m below the ground surface. The trench excavation shows similar soil stratum to the boring data from MAA Consultants [14]. Field sieve analysis was conducted to determine the grain size distribution curve, which is shown in Figure 4. Field investigation shows that the largest particle size of the site is up to 150 mm. The excavated materials were transported to laboratory to prepare reconstituted specimens.

3.2 Laboratory Cyclic Triaxial Test

Cyclic triaxial liquefaction tests were performed on reconstituted specimens with various gradation and relative density to establish the correlation among liquefaction resistance, gravels content, and initial relative density. Also, reconstituted specimens that are similar to field conditions were prepared to verify the cyclic resistance from

in situ BPT and V_s measurements. Because the largest grain size in the field is greater than 150 mm, in situ grain size distribution need be modified to fit in the cyclic triaxial apparatus, which is 150 mm in diameter. The Equivalent Weight Replacement Method, which maintains the portion finer than #4-sieve but reduce the maximum particle size to 25.4 mm, is used to prepare the reconstituted specimens. The simulation curve of grain size distribution using the Equivalent Weight Replacement method is also shown in Figure 4.

Reconstituted specimens are prepared by controlling total unit weight of specimens. The weights of oven-dry gravels and sands with simulation grain size distribution shown in Figure 4 for a specific unit weight are calculated and prepared respectively. Then, specific amount of gravels and sands are mixed and divided into five equal parts. The mixed gravelly sands are placed into a split mold and compacted to the designated relative density. After compaction, the compacted specimen was frozen for 3 hours. A frozen specimen surrounded by a rubber membrane was situated in the triaxial cell and subjected to 0.17 kgf/cm^2 isotropic pressure for erection.

To saturate reconstituted specimens, CO_2 is flushing through the specimen followed by deaired water after thawing. The completion of saturation is achieved when the measured B value exceeds 0.95. Then, the saturated specimen is consolidated isotropically. Cyclic loads are applied to the specimen in constant amplitude sine wave with fixed frequency 1.0 Hz by a MTS 810 system. The initial liquefaction is defined when the excess pore pressure ratio reaches 100% or the prescribed large deformation (4% axial strain) is developed.

Two series tests were performed to study the quantitative effects of liquefaction resistance of gravelly soils in terms of gravels content and relative density. The third test series that reconstruct the field compositions is used to verify the liquefaction

resistance evaluated by in situ index tests.

3.3 Large Hammer Penetration Test

Instrumented Large Hammer Penetration Test (LPT) system with strain gauges and accelerometers installed on the casing is implemented in this study. A pile driving analyzer is used to record the time histories of the strain on the casing and the acceleration of the ram. The peak force, peak velocity, and maximum transferred energy are calculated from the peak acceleration and the acceleration–time history. Five LPT tests were performed at 7 m spacing along the perpendicular direction to the river bank. Two boreholes (BH1, and 2) were penetrated using STK-41 steel casings (ASTM A36 steel) with 228.6mm in outer diameter and 31 mm in thickness. The other three boreholes (BH3, 4, and 5) were penetrated using steel casings of 168 mm in outer diameter and 40 mm in thickness.

3.4 In Situ and Laboratory Shear Wave Velocity Measurements

In situ shear wave velocity profile of the site is measured by Multi-channel analysis of surface wave (MASW) technique (Lin et al. [15]), one of the surface wave testing techniques. A 300 m survey line was performed to construct the 2-D shear wave velocity profile down to 30 m of the gravelly site.

There are few shear wave velocity measurements in liquefied gravelly sites. In addition, relationships among shear wave velocity and factors affecting liquefaction resistance of gravelly soils, such as gravel content, relative density, and state of stress, are not well defined in gravelly soils. To verify the in situ V_s measurement and assess the correlations between liquefaction resistance and V_s in gravelly soils, laboratory V_s

measurements in reconstituted specimens was performed in this study.

The laboratory V_s measurement instrumentation is illustrated schematically in Figure 5. Usually, a pair of bender elements is used to measure the shear wave velocity in laboratory. However, restricted by the gravels content, which retarded the installation of bender elements, and the large specimen size (30 cm in height), which required large source energy to be able to be sensed by the far end receiver, bender element configuration is not applicable. Alternatively, two 3-axis accelerometers are embedded on top and bottom plates of the cyclic triaxial apparatus. An internal mechanical impact device is designed to hit the side of the specimen to generate waves propagating both in up and down directions. Shear wave velocity is computed by the distance difference of top and bottom plates to the impact point divided by the time lag between the two horizontal-component accelerometers. Shear wave velocity measurements had been performed for different gradation, relative density, and state of stress.

4. RESULTS AND DISCUSSIONS

4.1 CRR from Cyclic Triaxial Liquefaction Tests

Three series of large-scale laboratory cyclic triaxial tests had been performed with 150 mm diameter reconstituted gravelly specimens to quantitatively assess the factors contributing to the cyclic liquefaction resistance and to estimate the liquefaction resistance of the testing site. Simplified procedure proposed by Seed and Idriss [16] implicitly assumes that the cyclic resistance of granular soil deposits is mainly influenced by the initial density and stress conditions. Evan and Zhou [13] reveal the significant contribution of gravels content to cyclic resistance of gravelly soils. Therefore, initial relative density (D_r) and gravel content (GC) should be

major factors that affect cyclic resistance of gravelly soils. Test series 1 and Test series 2 are conducted to quantitatively correlate the cyclic resistance of gravelly soils, expressed as cyclic resistance stress ratio (CRR), with gravels content and the initial relative density, respectively. Test series 3 was performed with reconstituted specimens similar to the field conditions to estimate the in situ cyclic resistance stress ratio of the site.

In test series 1, reconstituted specimens were prepared with a fixed relative density ($D_r=40\%$) but varied gravel contents ($GC=20\%$, 40% and 60%). Test series 2 used reconstituted specimens with a fixed gravel content ($GC=40\%$) and two initial relative densities ($D_r=20\%$ and 60%). The results from test series 1 are shown in Figure 6. Results from test series 1 and 2 are used to perform linear regression analysis to correlate the cyclic resistance stress ratios with respect to earthquake magnitude $M_w=7.5$, $CRR_{N1=15}$ (Seed et al. [17]), with gravel contents and the initial relative densities. The regression equation is expressed as:

$$CRR_{N1=15} = 0.0036 \times (GC\%) + 0.0050 \times (D_r\%) + 0.044 \dots\dots\dots (3)$$

The square of the correlation coefficient (R^2) is 0.958. The high R^2 value indicate that strong relationship exists among $CRR_{N1=15}$, the gravel content (GC), and the initial relative density (D_r).

In test series 3, specimens were prepared according to the gravel content and relative density obtained from trench exaction as shown in Table 1. The gravel content (GC) and the relative density (D_r) of the reconstituted specimens are 53% and 31% , respectively. The test results are also shown in Figure 6 along with results from test series 1 and Table 2. The result from Test series 3 shows that the correlation between the cyclic resistance stress ratio (CRR) and the number of loading cycles (NL) of the reconstituted specimens similar to the research site ($GC = 53\%$, $D_r = 31\%$) is

approximately equal to the curve of the specimens with $GC=40\%$ and $D_r = 40\%$. The $CRR_{N_1=15}$ value from figure 6 is 0.386, which is very close to the values calculated from equation 3 (0.39). The small difference between the two values indicates that equation 3 is a good approximation to $CRR_{N_1=15}$ in area with similar geologic deposits.

4.2 CRR from Large Hammer Penetration Tests (LPT)

At the Wufeng research site, five test boreholes using the Large Hammer Penetration technique were performed (3 boreholes with 168mm of outer diameter, and 2 boreholes with 228.6 mm of outer diameter) and the results of blow counts (N_b) are shown in Table 3. The ground water table was 2.9 m below ground surface when the tests were performed. Because N_b values between 2 to 8 m deep from ground surface are significantly lower than those deeper than 8 m, possibly liquefied stratum is located between 3 to 8 m below ground surface.

The relationship between the dynamic energy and the potential energy is used to obtain the hammer efficiency. After correcting for the energy using equation 1 (Sy and Campanella [9]), the corrected LPT blow count (N_{b30}) is calculated, and the SPT- N_{60} value obtained from the LPT- N_{b30} and SPT- N_{60} correlation curve, as shown in Figure 7, is used to estimate CRR. The $CRR_{7.5}$ from LPT test is tabulated at Table 4.

4.3 CRR from In Situ and Laboratory Shear Wave Velocity Measurement

A 300 m survey line was performed to construct the shear wave velocity profile down to 30 m of the gravelly site using MASW technique. Shear wave velocity profile using MASW is shown in Figure 8 (Lin et al. [15]). The V_s -profile indicates that the lower V_s were detected between 2 to 7 m from ground surface, which is consistent with the LPT results.

In order to compare with the results from triaxial cyclic tests, the shear wave velocities of specimens for Test series 1 and 2 were measured prior to conducting cyclic loading by internal shear wave velocity instrumentation system. The results are shown in Figure 9, which indicate shear wave velocity increases with the increase of the confining pressure, relative density, and gravel content. Based on results from cyclic triaxial test, CRR of reconstituted specimens prepared in field conditions (GC = 53%, $D_r = 31\%$) is close to that of the specimen with GC=40% and $D_r = 40\%$. Therefore, the in situ shear wave velocity should be approximate to laboratory measured V_s from specimen with GC=40% and $D_r = 40\%$. The laboratory measured V_s from specimen with GC=40% and $D_r = 40\%$ at confining stress 1 kg/cm^2 is 215, which is reasonably agree with the in situ V_s at 5 m deep (190 ~ 230 m/s).

4.4 Verification of CRR Based on Field Observation

To verify the CRR from cyclic triaxial tests, LPT, and V_s approaches. Field observations after the Chi-Chi earthquake at the site (Lin and Chang [18]) are compared with the factor of safety from cyclic stress approach developed by Seed and Idriss [15]. The cyclic stress ratio induced by earthquake (CSR) is computed by:

$$CSR = \left(\frac{\tau_{av}}{\sigma'_o} \right)_{eq} = 0.65 \cdot \left(\frac{a_{max}}{g} \right) \cdot \left(\frac{\sigma_v}{\sigma'_v} \right) \cdot r_d \dots\dots\dots (4)$$

where a_{max} = maximum horizontal ground acceleration, σ_v, σ'_v = total and effective overburden pressures, respectively, r_d = stress reduction factor, and g = gravity acceleration. The recorded maximum horizontal acceleration near the site is 0.79g (Lin and Chang [18]). Cyclic resistance stress ratio, CRR, are determined from cyclic triaxial tests (Seed et al [4]), LPT-based (equation 1 and Harder and Seed [8]), and V_s -based (Andrus and Stokoe [6]) approaches. The factor of safety against

liquefaction is:

$$FS = \frac{CRR}{CSR} \dots\dots\dots (5)$$

A factor of safety less than 1 indicates liquefaction occurred.

To compute CRR based on cyclic triaxial tests, correction factors for stress reversal in cyclic triaxial tests (Seed and Peacock [19]) and multidirectional shaking (Seed et al. [20]) are applied. CRR from cyclic triaxial tests is computed by:

$$CRR = 0.572 \cdot \left(\frac{\sigma_d}{2\sigma'_c} \right)_{tri} \dots\dots\dots (6)$$

where σ_d = deviator stress and σ'_c = effective confining pressure.

The CRR computed by cyclic triaxial tests is 0.22 for $CRR_{NL=15}$ equal to 0.386. The CSR computed by equation 4 at depth 4.5m is 0.32. Therefore, the factor of safety from cyclic triaxial tests is 0.69. The result indicates the gravelly soil liquefied, which agrees with the field observation.

Incorporate equation 1, correlation of Figure 7, and correlation between CRR and SPT- N_{60} suggested by Youd et al. [21], CRR can be evaluate from LPT data. The factors of safety against liquefaction for the 5 LPT-boreholes are shown in Figure 10. The results indicate that liquefaction could occur from 3 to 8 m below surface. This is reasonably consistent with the results of the laboratory cyclic triaxial tests, and the liquefaction evidences observed at the research site. However, the factors of safety computed by the LPT approach are generally smaller than those from cyclic triaxial tests.

In situ shear wave velocities are analyzed using the procedure proposed by Andrus and Stokoe [6]. The factors of safety against liquefaction are shown in Figure 11. The factors of safety computed from shear wave velocity data vary

similarly to results from LPT and cyclic triaxial tests. Soil liquefaction could occur between 3 to 8 m deep from surface. Also, the factor of safety from V_s agrees better with factor of safety of cyclic triaxial tests.

5. CONCLUSION AND SUGGESTION

A liquefied gravelly deposit site during the Chi-Chi earthquake was selected for this research. Instrumented Large Hammer Penetration Test (LPT) and shear wave velocity (V_s) measurements were performed to evaluate the liquefaction resistance of gravelly soils. In addition, large-scale cyclic triaxial tests on reconstituted gravelly soil specimen (15 cm in diameter and 30 cm in height) were conducted. The three correlations for characterizing liquefaction resistance of gravelly soils are compared with field observation results. The important conclusions are discussed below:

1. The corrected Large Hammer blow count only considers the effect of the total casing frictional force. Therefore, the wave equation should be used to calculate the effect of the casing side friction to produce a better LPT analysis in assessing the liquefaction potential of the gravelly soil.
2. Based on results of cyclic triaxial tests with reconstituted gravelly specimens, a regression model (equation 3) had been developed to estimate cyclic resistance stress ratio (CRR) in terms of the gravel content and the initial relative density. The model had been verified by both field observations and laboratory tests.
3. Liquefaction resistances estimated by blow counts of energy-corrected Large Hammer Penetration tests agree well with field observed evidences and results from cyclic triaxial tests. However, factors of safety computed by LPT are generally smaller than CRR from cyclic triaxial tests.
4. In situ shear wave velocity measurements using the surface wave propagation technique on gravelly deposits had been performed. The comparison between the

in situ and laboratory V_s measurements indicates the difference is minor. Therefore, reliable in situ V_s measurements on gravely deposits using nondestructive, non-intrusive techniques are promising.

5. Correlation between CRR of gravely soils and V_s proposed by Andrus and Stokoe [6] has been tested by field evidences and cyclic triaxial tests. The results show that the correlation agrees well with field observation. Also, CRR based on V_s are closer to CRR from cyclic triaxial test compared with CRR from LPT.
6. Although LPT- and V_s -based approaches generally performed well in this study, the small values of factor of safety indicate both approaches need be further refined.
7. Research data and papers related to Large Hammer Penetration Test are limited because the Large Hammer Penetration technique is a new development. Further research on the relationship between gravelly soil and liquefaction should be performed by drilling additional LPT boreholes at several liquefied gravelly soil deposits to establish a more reliable method for liquefaction potential assessment.

Acknowledgements

Funding for this research was provided by the National Science Council of ROC under contracts No. NSC 91-2211-E-005-021.

REFERENCES

- [1] Chu, B.L., Hsu, S.C., Lai, S.E., Chang, M.J. Soil Liquefaction Potential Assessment of the Wufeng Area after the 921 Chi-Chi Earthquake. Report of National Science Council. 2000. (in Chinese)
- [2] Yegian M. K., Ghahraman V. G., and Harutiunyan R. N. Liquefaction and Embankment Failure Case History, Armenia Earthquake. Journal of the Geotechnical and Geoenvironmental Engineering, ASCE 1988; 120(3): 581-596.
- [3] Seed, H.B. and Lee, K. L. Liquefaction of Saturated Sands during Cyclic Loading. Journal of the Soil Mechanics and Foundation Division, ASCE 1966; 92(6): 105-134.
- [4] Seed, H. B., Tokimatsu, K., Harder, L. F., and Chung, R. M. Influence of SPT Procedures in Soil Liquefaction Resistance Evaluations. Journal of Geotechnical Engineering, ASCE 1985; 111(12): 1425-1445.
- [5] Robertson, P. K., and Wride, C. E. Evaluating Cyclic Liquefaction Potential Using the Cone Penetration Test. Canadian Geotech. Journal 1998; 35(3): 442–459.
- [6] Andrus, R. D., Stokoe, K. H. II Liquefaction Resistance of Soils from Shear-wave Velocity. Journal of Geotechnical and Geoenvironmental Engineering, ASCE 2000; 126(11): 1015-1025.
- [7] Harder, L. F. Application of the Becker Penetration Test for Evaluating the Liquefaction Potential of Gravelly Soils. Proceedings of the NCEER Workshop on Evaluation of Liquefaction Resistance, Salt Lake City, Utah, 1997.
- [8] Harder, L.F., Seed, H.B. Determination of Penetration Resistance for Coarse-grained Soils Using the Becker Hammer Drill. Report No. UBC/EERC-86/06, Earthquake Engineering Research Center, Univ. of California

at Berkeley. 1986.

- [9] Sy A. and Campanella R.G. Becker and Standard Penetration Tests (BPT-SPT) Correlations with Consideration of Casing Friction. *Canadian Geotech. Journal* 1994; 31: 343-356
- [10] GRL and Associates, Inc. CAPWAP Manual. Cleveland, Ohio. 1993.
- [11] Kokusho, T., Yoshida, Y., and Tanaka, Y. Shear Wave Velocity in Gravelly Soils with Different Particle Gradings. In: M. D. Evans and R. J. Frigaszy, eds. *Static and Dynamic Properties of Gravelly Soils*. New York: Geotech. Spec. Publ. No. 56. ASCE, 1995: 92–106.
- [12] Evans, M. D., Seed, H. B., and Seed, R. B. Membrane compliance and liquefaction of sliced gravel specimens. *Journal of Geotechnical Engineering*, ASCE 1992; 118(6): 856-872.
- [13] Evans, M. D. and Zhou, S. Liquefaction Behavior of Sand-Gravel Composites. *Journal of Geotechnical Engineering*, ASCE 1994; 121(3): 287-298.
- [14] MAA Consultant Engineers, Inc. Investigating the Soil Liquefaction Phenomenon in Nantou and Wufeng. Report of National Science Council, 2000.
- [15] Lin C.P., Chang, C.J., and Lin, J.E. The application of Shear Wave Velocity to the Liquefaction Assessment in Central Taiwan. *Proc. of Conference on the Liquefaction Potential Assessment of Central Taiwan*. 2002: D-1-D-24.
- [16] Seed, H.B., and Idriss, I.M. Simplified Procedure for Evaluating Soil Liquefaction Potential. *Journal of the Soil Mechanics and Foundations Division*, ASCE 1971; 97(SM9): 1249-1273.
- [17] Seed, H. B., Tokimatsu, K., Harder, L. F., and Chung, R. M. Influence of SPT Procedures in Soil Liquefaction Resistance Evaluations. *Journal of*

Geotechnical Engineering, ASCE 1985; 111(12): 1425-1445.

- [18] Lin, P.S. and Chang, C.W. Damage Investigation and Liquefaction Potential Analysis of Gravelly Soil. Journal of the Chinese Institute of Engineers 2002; 25(5): 1-11.
- [19] Seed, H. B. and Peacock, W. H. Test Procedure for Measuring Soil Liquefaction Characteristics. Journal of the Soil Mechanics and Foundations Division, ASCE 1971; 97(SM8): 1099-1119.
- [20] Seed, H. B., Lee, K. L., Idriss, I. M., and Markdisi, F. I. Representation of Irregular Stress Time Histories by Equivalent Uniform Stress Series in Liquefaction Analyses. Report No. UBC/EERC-75-29, Earthquake Engineering Research Center, Univ. of California at Berkeley. 1975.
- [21] Youd, T. L. et al. Liquefaction Resistance of Soils: summary report from the 1996 NCEER and 1998 NCEER/NSF workshops on evaluation of liquefaction resistance of soils. Journal of Geotechnical and Geoenvironmental Engineering, ASCE 2001; 127(10): 817-833.

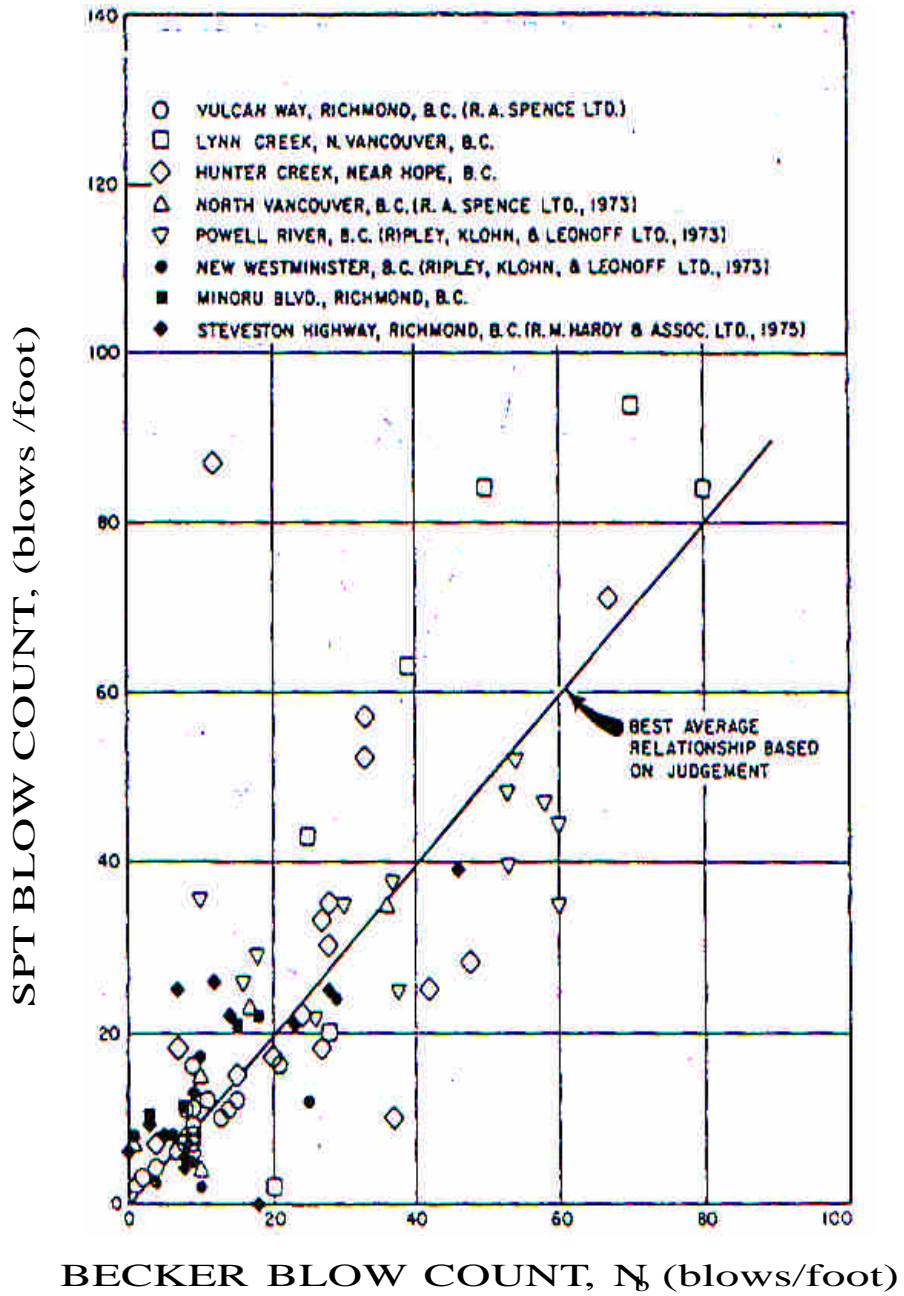


Figure 1. Relationship between BPT- N_b and SPT-N

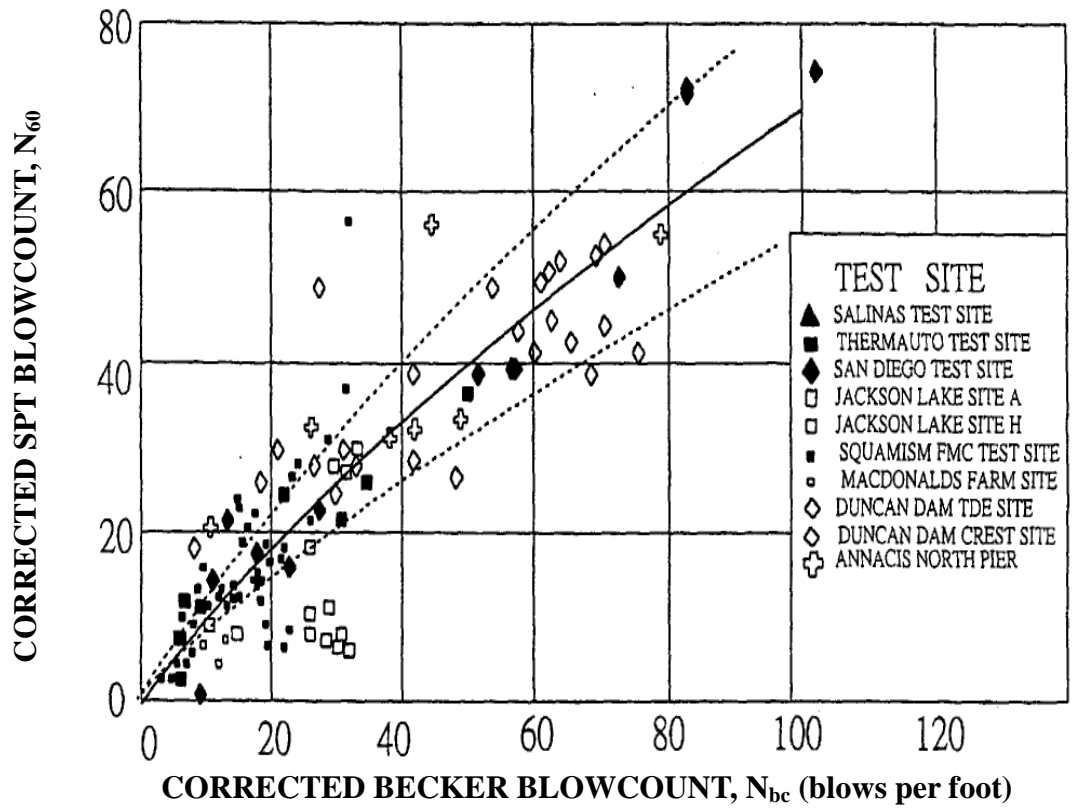


Figure 2. Relationship between SPT- N_{60} and BPT- N_{bc} (Harder and Seed [8])

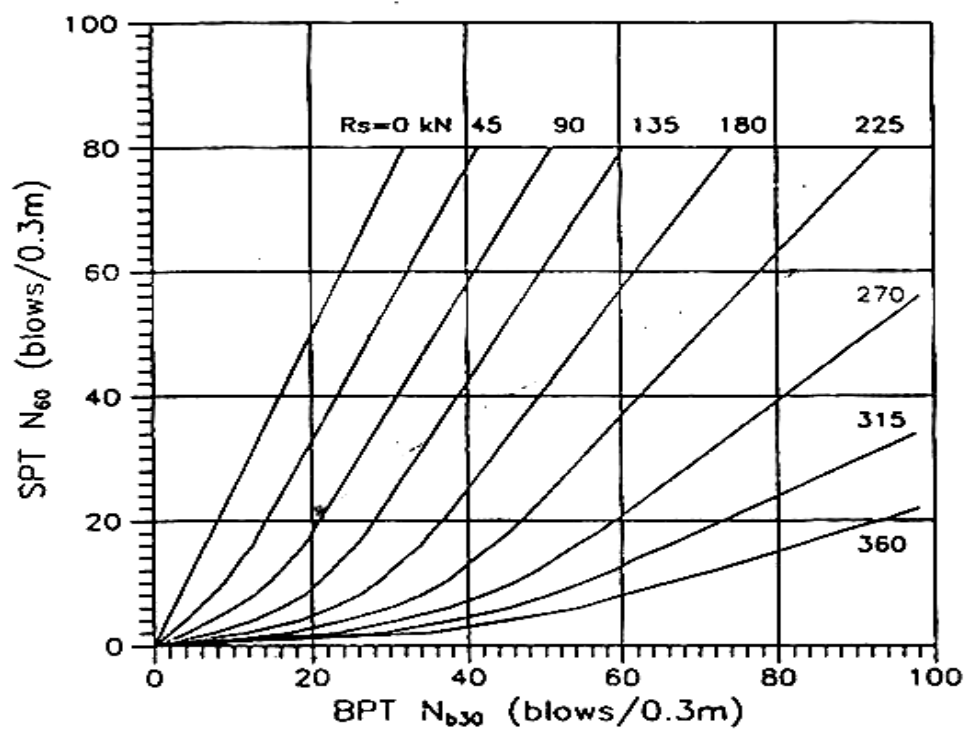


Figure 3. Correlation of Casing Frictional Force, BPT- N_{b30} and SPT- N_{60} (Sy and Campanella [9])

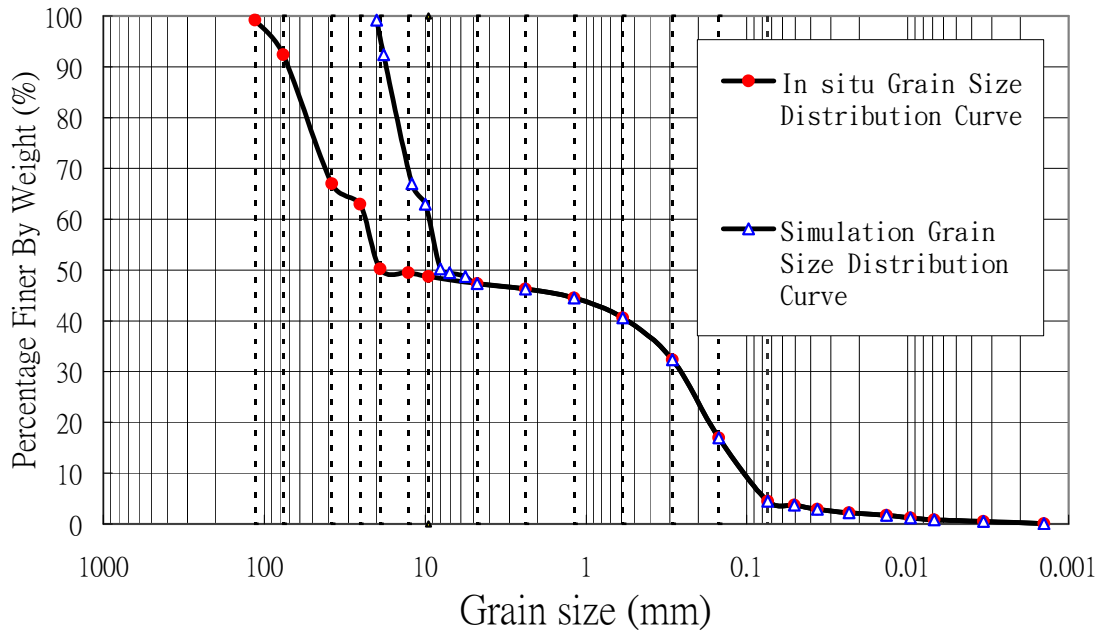


Figure 4. Grain Size Distribution Curves of in situ and reconstituted specimen

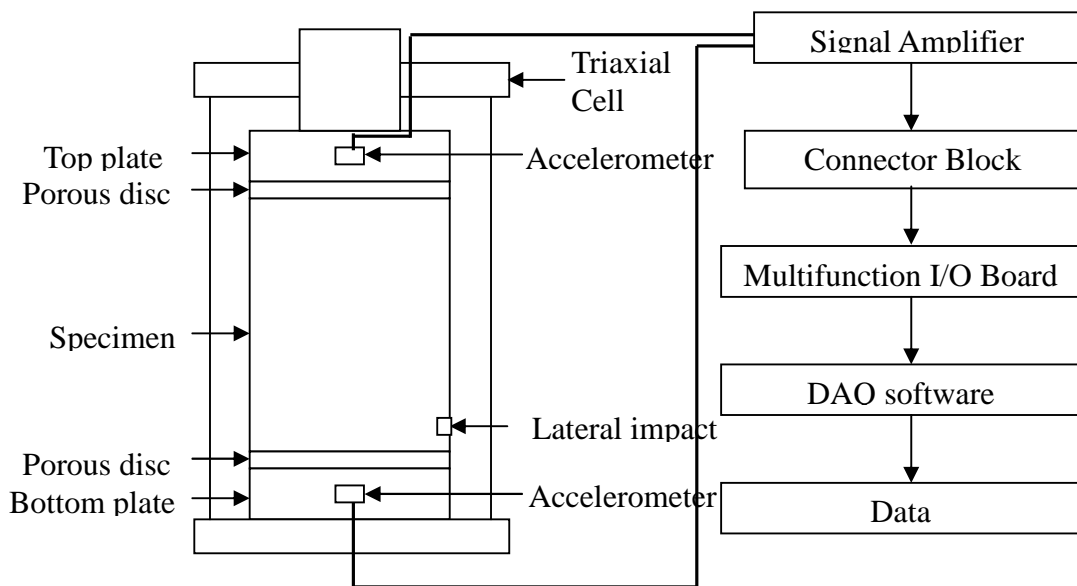


Figure 5. The Instrumentation of Schematic diagram of experimental setup for laboratory shear wave velocity.

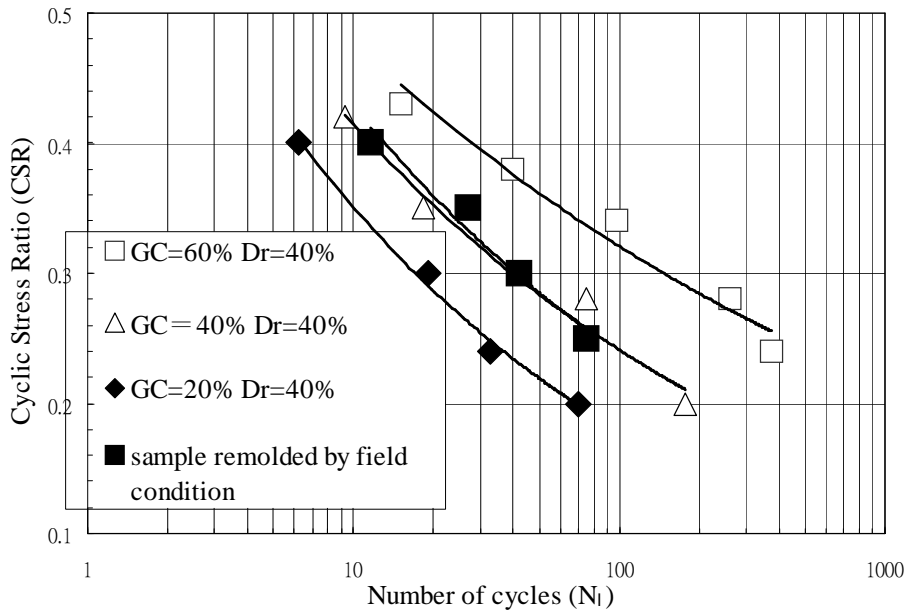


Figure 6. Relationship between the Cyclic Stress Ratio (CSR) and the Number of Cycles (N_1) of the Reconstituted Specimens

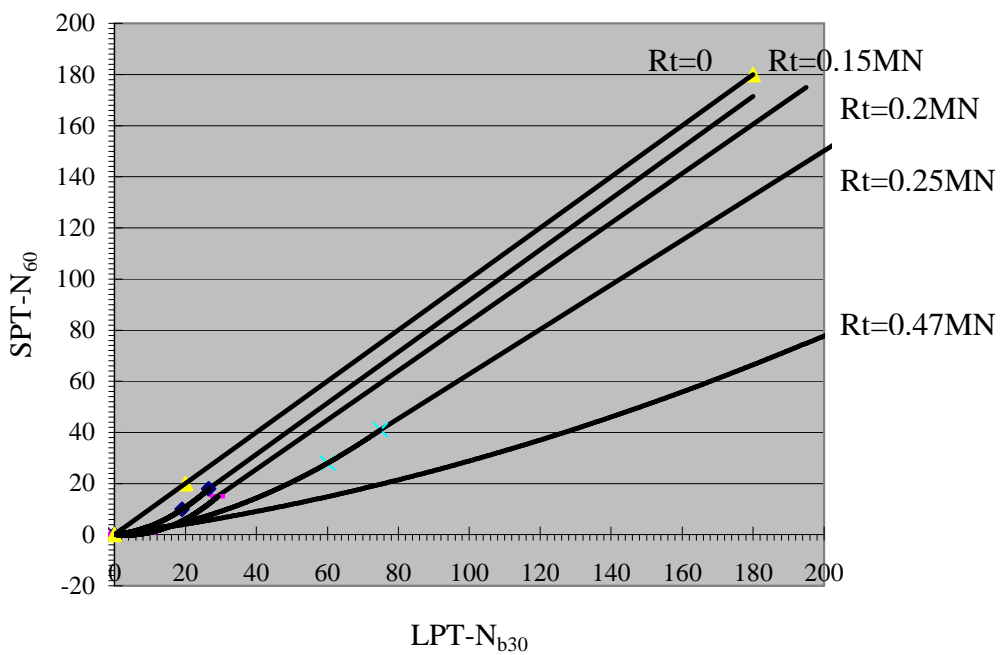


Figure 7. Correlations of Total Casing Frictional Forces (Rt), LPT- N_{b30} , and SPT- N_{60} of the Testing Site

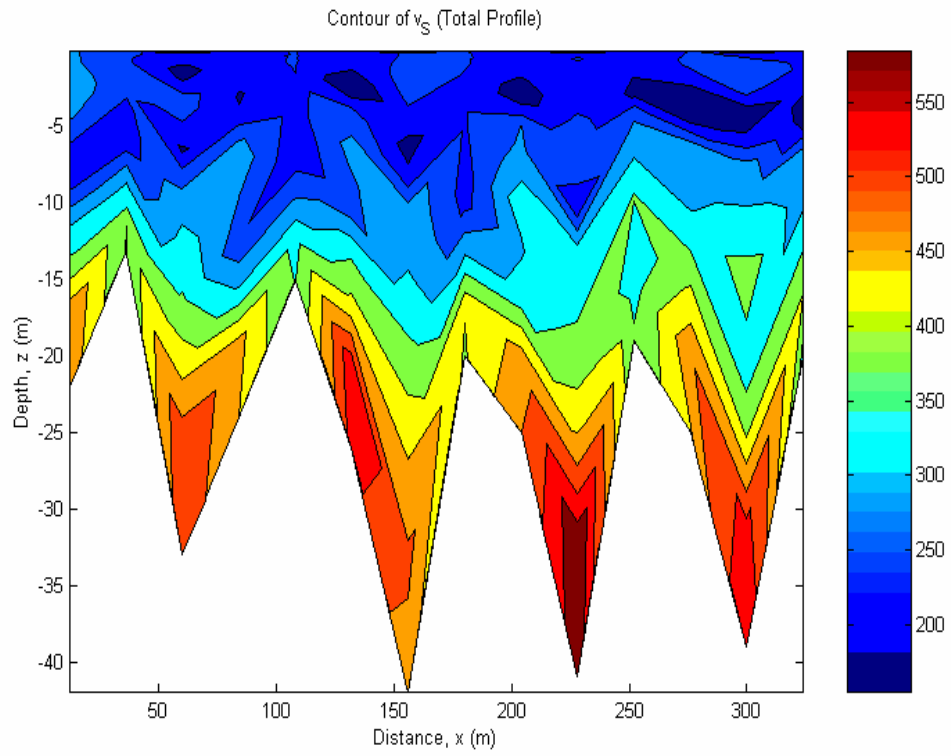


Figure 8. V_s -Profile near the Wufeng Research Site (Lin,et al.[15])

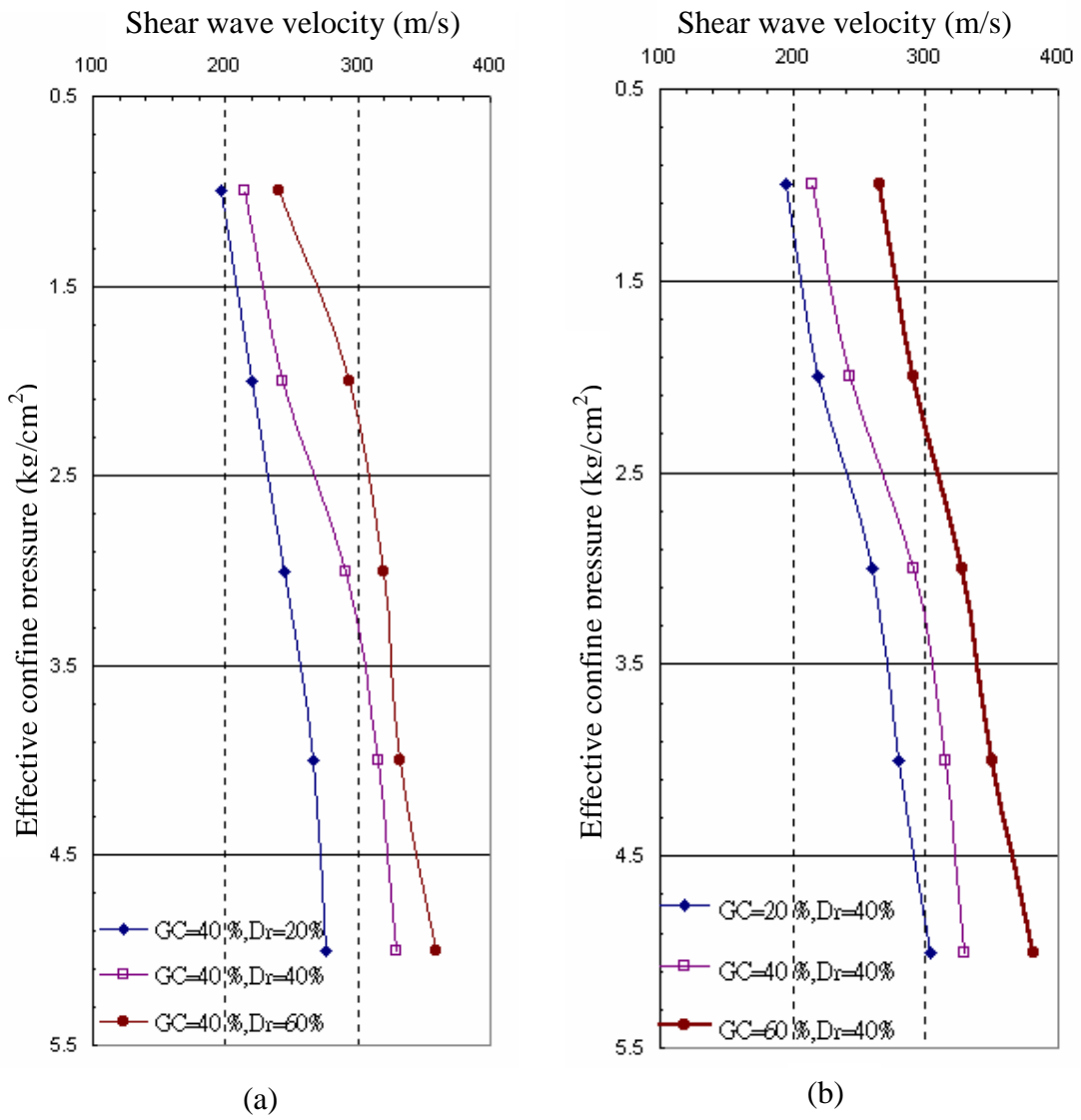


Figure 9. Variation of shear wave velocity and confining pressure (a) GC=40%, Dr=20, 40, and 60%, and (b) GC=20, 40,60%, Dr=40%

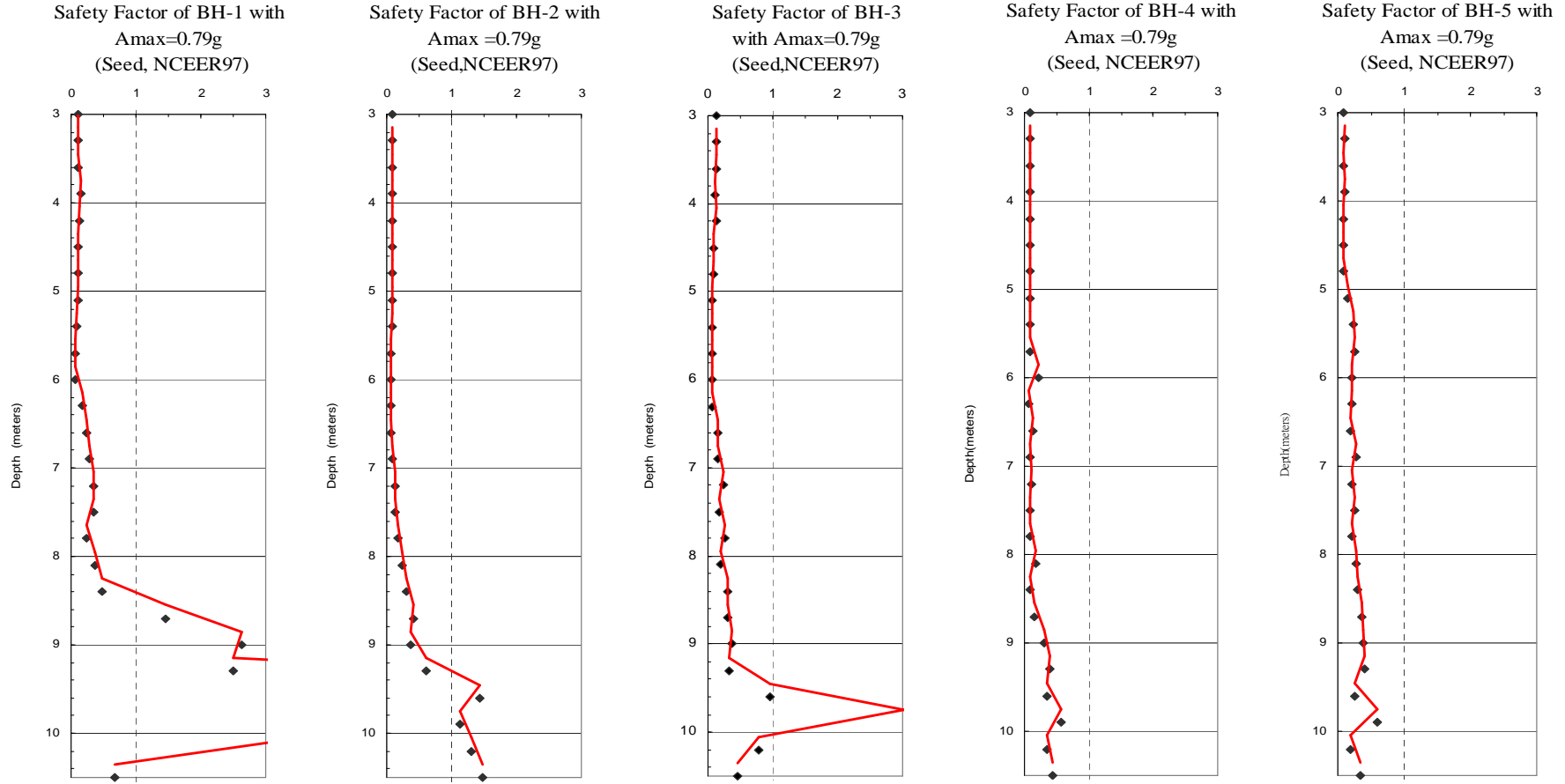


Figure 10. Factor of Safety from instrumented LPT tests under $a_{max}=0.79g$.

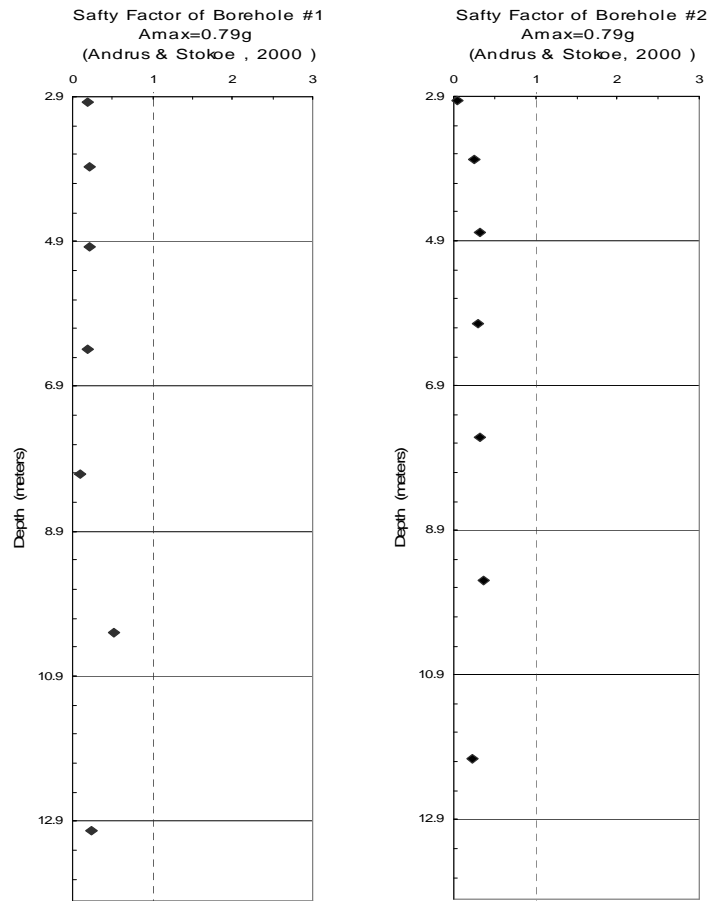


Figure 11. Factor of Safety from In Situ Shear Wave Velocity Measurement

Table 1. Soil Profile in the Trench Excavation

Location: Fu Tin Bridge in Wufong County			Water Table: -4.5 m				The General Physical Test of the soil			
Depth (m)	Boring figure	Description of soil Profile	Grain size(%)				USCS	γ (g/cm ³)	W _n (%)	G _s
			Gravel	Sand	Silt	Clay				
-0.5	SF	Gravel and much yellowish gray fine sand								
-1.5	GP	Gravelly layer; contains yellow coarse sand in very loose state	53	44	3	0	GP	1.99	7.24	2.67
-2.5										
-3.5										
-4.5	cl	Occasionally with yellow silty clay and gravel								
-5.5	GP	Gravelly layer; contains much greyish coarse sand in very loose state								
-6.5										

Table 2. Cyclic Triaxial Test Results of Specimens Reconstituted in Field Condition

Name of Test	Reconstituted soil GC=53% Dr=31%			
	1	2	3	4
No. of Specimen				
Dry Density γ_d (g/cm ³)	1.85			
Specific Gravity, G _s	2.71			
Relative Density, D _r (%)	31			
Void Ratio, e _o	0.54			
Coeff. of Uniformity, C _u	99			
Coeff. of Curvature, C _d	0.0792			
Effective Grain Size, D ₁₀ (mm)	0.1			
Mean Grain Size, D ₅₀ (mm)	8			
USCS	GP			
Cyclic Stress Ratio, CSR	0.4	0.35	0.3	0.25
No. of Initial Liquefaction, N ₁	12	27	42	75
CSR of NL=15	0.386			

Table 3. The Blow Counts (N_b) of the Large Penetration Tests (GL=- 2.9m)

Borehole No.	BH-1	BH-2	BH-3	BH-4	BH-5	Borehole No.	BH-1	BH-2	BH-3	BH-4	BH-5
Casing Dia. (mm)	228.6	228.6	168.0	168.0	168.0	Casing Dia.(mm)	228.6	228.6	168.0	168.0	168.0
Depth(cm)	Blow Counts (N_b)					Depth(cm)	Blow Counts (N_b)				
30				1		930	37	33	22	32	26
60		4		3		960	39	40	37	31	21
90		4		4		990	39	36	29	36	33
120		3		3	5	1020	37	34	31	31	21
150		3	9	4	6	1050	30	35	25	24	20
180		3	11	5	11	1080	20	35	30	16	20
210		3	13	2	6	1110	21	34	19	16	25
240	4	2	15	1	5	1140	22	37	13	24	22
270	2	2	14	1	1	1170	47	29	16	30	25
300	2	1	4	1	1	1200	45	25	14	37	28
330	3	1	5	1	2	1230	48	27	14	22	34
360	4	0.5	5	0.5	1	1260	50	15	10	12	33
390	7	0.5	4	0.5	3	1290	46	13	5	5	30
420	6	1	5	0.5	1	1320	42	14	4	4	33
450	4	1	2	0.5	0	1350	55	24	2	21	28
480	5	2	0.5	1	5	1380	86	64	4	32	27
510	5	2	0.5	2	12	1410	67	56	10	39	32
540	3	3	0.5	3	15	1440	51	45	28	40	38
570	1	1	0.5	5	17	1470	42	33	27	40	48
600	1	1	0.5	12	16	1500	38	25	28	60	49
630	10	2	1	11	14	1530	45	27	26	50	37
660	14	3	11	10	15	1560	74	41	29	41	43
690	16	5	9	5	18	1590	65	47	30	44	33
720	20	13	15	8	19	1620	40	71	48	42	37
750	20	13	15	16	21	1650	43	74	57	62	22
780	14	12	13	11	18	1680	34	77	49	57	
810	21	15	12	10	22	1710	37	103	45	50	
840	25	20	20	3	22	1740	33	110	76	51	
870	35	26	22	11	25	1770	32	136	82		
900	37	27	24	22	25	1800					

Table 4. Cyclic Resistance Stress Ratio from LPT Test

Borehole No.	BH-1	BH-2	BH-3	BH-4	BH-5	Borehole No.	BH-1	BH-2	BH-3	BH-4	BH-5
Casing Dia. (mm)	228.6	228.6	168.0	168.0	168.0	Casing Dia. (mm)	228.6	228.6	168.0	168.0	168.0
Depth(cm)	F.S.(0.79g)					Depth(cm)	F.S.(0.5g)				
30				1.52		30				1.55	
60		1.50		1.51		60		1.54		1.55	
90		1.50		1.52		90		1.55		1.55	
120		1.51		1.50	1.50	120		1.55		1.53	1.53
150		1.50	1.46	1.50	1.46	150		1.54	1.52	1.54	1.42
180		1.50	1.51	1.46	1.50	180		1.54	1.53	1.50	1.54
210		1.42	1.37	1.46	1.36	210		1.46	1.50	1.50	1.49
240	1.15	1.21	1.45	1.24	1.15	240	1.36	1.40	1.51	1.43	1.36
270	1.02	1.08	1.14	1.20	1.07	270	1.36	1.36	1.36	1.40	1.36
300	0.10	0.10	0.13	0.09	0.09	300	0.16	0.15	0.20	0.15	0.15
330	0.11	0.09	0.14	0.09	0.10	330	0.17	0.14	0.22	0.14	0.15
360	0.11	0.09	0.13	0.09	0.09	360	0.18	0.13	0.21	0.13	0.14
390	0.16	0.08	0.11	0.08	0.10	390	0.26	0.13	0.17	0.13	0.16
420	0.13	0.08	0.12	0.08	0.08	420	0.22	0.13	0.19	0.13	0.13
450	0.10	0.08	0.09	0.08	0.08	450	0.16	0.13	0.13	0.12	0.12
480	0.11	0.08	0.08	0.08	0.09	480	0.18	0.13	0.12	0.12	0.14
510	0.11	0.08	0.07	0.08	0.15	510	0.17	0.13	0.12	0.13	0.24
540	0.09	0.09	0.07	0.09	0.23	540	0.14	0.14	0.12	0.14	0.36
570	0.07	0.07	0.07	0.08	0.26	570	0.12	0.12	0.11	0.13	0.41
600	0.07	0.07	0.07	0.22	0.22	600	0.11	0.11	0.11	0.35	0.34
630	0.18	0.07	0.07	0.08	0.21	630	0.29	0.11	0.11	0.12	0.33
660	0.24	0.07	0.15	0.12	0.20	660	0.39	0.12	0.24	0.19	0.32
690	0.27	0.08	0.15	0.08	0.28	690	0.44	0.13	0.23	0.12	0.44
720	0.35	0.13	0.23	0.12	0.21	720	0.56	0.21	0.37	0.18	0.33
750	0.35	0.13	0.18	0.09	0.25	750	0.55	0.20	0.28	0.14	0.39
780	0.24	0.18	0.25	0.08	0.22	780	0.37	0.28	0.40	0.13	0.35
810	0.36	0.25	0.19	0.17	0.27	810	0.57	0.39	0.30	0.26	0.43
840	0.47	0.31	0.30	0.08	0.29	840	0.75	0.49	0.47	0.12	0.46
870	1.47	0.42	0.29	0.16	0.37	870	2.32	0.66	0.47	0.26	0.59
900	2.63	0.37	0.36	0.31	0.37	900	4.15	0.58	0.57	0.48	0.59